Title
Functional and structural dissection of an N-terminal domain in the anti-apoptotic protein Bc12

Author
Lee, Lillian C.

Publication Date
1996

Peer reviewed|Thesis/dissertation

Functional and Structural Dissection of an N-Terminal Domain in the Anti-Apoptotic Protein Bcl2

by

Lillian C. Lee

A Thesis

Submitted in partial satisfaction of the
requirements for the M.D. with Thesis Program
of the
University of California, San Francisco

ABSTRACT

A region occupying approximately 24 amino acids near the N terminus of human Bcl2 is essential for this cytoplasmic membrane protein's ability to inhibit apoptosis. Systematic mutagenesis of this N-terminal region indicates that only five hydrophobic and aromatic residues within it are specifically required for function. Computerized secondary structure prediction, together with circular dichroism spectroscopy of synthetic peptides, indicate that the region encompassing these five residues has the propensity to take on an α-helical conformation in the presence of SDS micelles, which presumably mimic the hydrophobic surfaces of cellular membranes or polypeptides. The five critical residues are predicted to be clustered on one face of this putative helix, where they might serve to mediate protein/protein contacts involved in the multimerization of Bcl2 or in the interaction of Bcl2 with other, as-yet-unidentified components of the apoptotic pathway. Apparent structural homologues of this helical motif are also present in at least some other anti-apoptotic proteins from the Bcl2 family, but not in those family members that tend to potentiate, rather than inhibit, apoptosis.

TABLE OF CONTENTS

LIST OF TABLES AND FIGURES

INTRODUCTION

All differentiated cells in multicellular organisms appear to be able to carry out their own death through the activation of an internally encoded death program. When activated, the program initiates a characteristic form of cell death called apoptosis. Cells that are produced in excess, that have developed improperly, or that have sustained genetic damage may be eliminated through apoptosis. This form of physiologic cell death may be distinguished from the other principal mechanism of cell death, namely pathologic cell death or necrosis. The cellular events involved in necrotic cell death include the loss of osmotic equilibrium, cell swelling, and the rupture of intracellular contents into the extracellular milieu, with a subsequent inflammatory cell response. Apoptosis involves a different constellation of characteristic morphologic changes, including cell shrinkage, plasma membrane blebbing, nuclear fragmentation, and chromatin condensation (reviewed in Ref. 1). In addition, alterations in the plasma membrane of the apoptotic cell signal neighboring viable cells to engulf them, thereby eliminating the dying cell from the extracellular environment and avoiding an inflammatory reaction.

Though the conditions necessary to trigger apoptosis differ among cell types, the underlying biochemical pathway is thought to be evolutionarily conserved. Most details of this pathway are not known, but recent studies suggest that critical early steps take place within the cytoplasm (2), and that certain highly conserved cytoplasmic proteins participate in the response. In particular, the propensity of cells to undergo apoptosis appears to be controlled by a family of structurally-related cytoplasmic proteins whose prototype is the human *bcl2* gene product (reviewed in Refs. 3 and 4). The

gene *bcl2* was first identified in studies of a chromosomal anomaly that occurs in the vast majority of cases of follicular non-Hodgkin's lymphoma. The anomaly consists of a translocation of genetic material between the long arms of chromosomes 14 and 18, known as t(14,18). This translocation juxtaposes the *bcl2* gene with transcription control elements associated with the immunoglobulin heavy chain locus, resulting in deregulation of *bcl2* expression. Overexpression of *bcl2* in cell lines extends cellular survival without inducing proliferation by inhibiting apoptosis. The *bcl2* gene product is a 239-amino-acid cytoplasmic integral membrane protein with a wide tissue distribution. When expressed at high levels, it can be shown to associate with mitochondrial membranes, the nuclear envelope, and the endoplasmic reticulum. The significance of these associations is uncertain and, at present, neither the physiologic site nor mechanism of Bcl2 action is known.

Studies in other vertebrates, as well as in nematodes and animal viruses, have identified an assortment of proteins that share regions of significant sequence homology with Bcl2. When over-expressed individually in cells, some of these exhibit anti-apoptotic activity similar to that of Bcl2, whereas others strongly promote apoptosis and still others modulate the response in a variable manner. Several of these proteins have been found to form dimers or higher oligomers with themselves and with one another (5-11), and there is evidence that such interactions among Bcl2 family members are important for their biological effects (11,12).

The biological function of Bcl2 was discovered by finding that it allowed interleukin-3-dependent cells to resist death upon withdrawal of the cytokine (13). The cells expressing Bcl2 entered a quiescent (G_o) state in which they survived for many days, but they readily reentered the cell cycle upon

addition of cytokine. Now numerous examples exist in which apoptotsis due to external toxic stimuli can be rescued by Bcl2 (Table 1). Despite numerous positive examples, Bcl2 does not prevent every cell death. In particular, it does not have a substantial effect on negative selection of thymocytes (14) and does not easily prevent apoptosis in targets of cytotoxic T-cell killing (15). However, Bcl2 can occasionally affect outcomes by these stimuli, suggesting that results can be dose-related. The fact that Bcl2 can inhibit apoptosis resulting from so many different signals and intracellular pathways implies that it must act after the convergence of many signals in the apoptotic pathway (Fig. 1). However, because it cannot countermand all death signals, it is possible that more than one distal pathway of apoptosis exists. Alternatively, individual Bcl2 family members may prove more effective in certain contexts than others.

Site-directed mutagenesis studies have delineated at least three discrete functional regions within human Bcl2 (11,16-19). A hydrophobic domain at the C terminus (residues 203-239) confers membrane anchorage; deletion of this region reduces but does not eliminate Bcl2 activity (6,16,17), perhaps because the mutant retains the ability to associate with membrane-bound family members. By contrast, activity can be completely eliminated by mutations in a second region (residues 90-203) that includes a pair of sequence motifs (termed BH1 and BH2) which are known to be required for Bcl2 homo- and heterodimerization (11,16,17). The third region, located near the N terminus within residues 6-31, is also essential for activity: Bcl2 deletants which lack this region not only fail to prevent apoptosis (16,17) but can also function as *trans*-dominant inhibitors of wild-type Bcl2 (17). In this report, the results of a detailed analysis of this N-terminal region of human Bcl2 are presented. The functional testing of Bcl2 missense mutants which reveals the

Table 1. Cell Deaths Repressed by Bcl2

- Lymphoid
  - Factor withdrawal -- IL-2, IL-3, IL-4, IL-6, GM-CSF
  - Glucocorticoids
  - γ Irradiation
  - Phorbol esters
  - Calcium
  - Cross-linking by anti-CD3
- Neuronal
  - Factor withdrawal -- NGF, BDNF, Neurotrophin-3
  - Serum withdrawal
  - Calcium
  - Infarction
  - Axotomy
  - Naturally occurring cell death
- Fibroblasts
  - Serum deprivation and MYC induction
- Oncogene-related
  - MYC-induced
  - E1A-induced
  - p53-mediated
- Viral infections
  - Adenovirus
  - Sindbis virus
  - HTLV-1
- Chemotherapeutic drugs
  - DNA synthesis inhibitors
  - Alkylating agents
  - Topoisomerase inhibitors
  - Microtubule inhibitors
  - Antimetabolites
- Oxidant stress
  - Hydrogen peroxide
  - Menadione
  - Membrane peroxidation
- Others
  - TGF-β
  - Staurosporine
  - Loss of extracellular matrix

Figure 1. Schematic of the cell death pathway. Various stimuli generate a cell death signal. The ratio of heterodimers of the cell death regulators determine the susceptibility to death, and cell death effects execute programmed cell death. The precise intermediate steps and the critical protease substrates are not known. (Taken from Yang, E. and Korsmeyer, S.J. (1996)*Blood* **88**, 386-401)

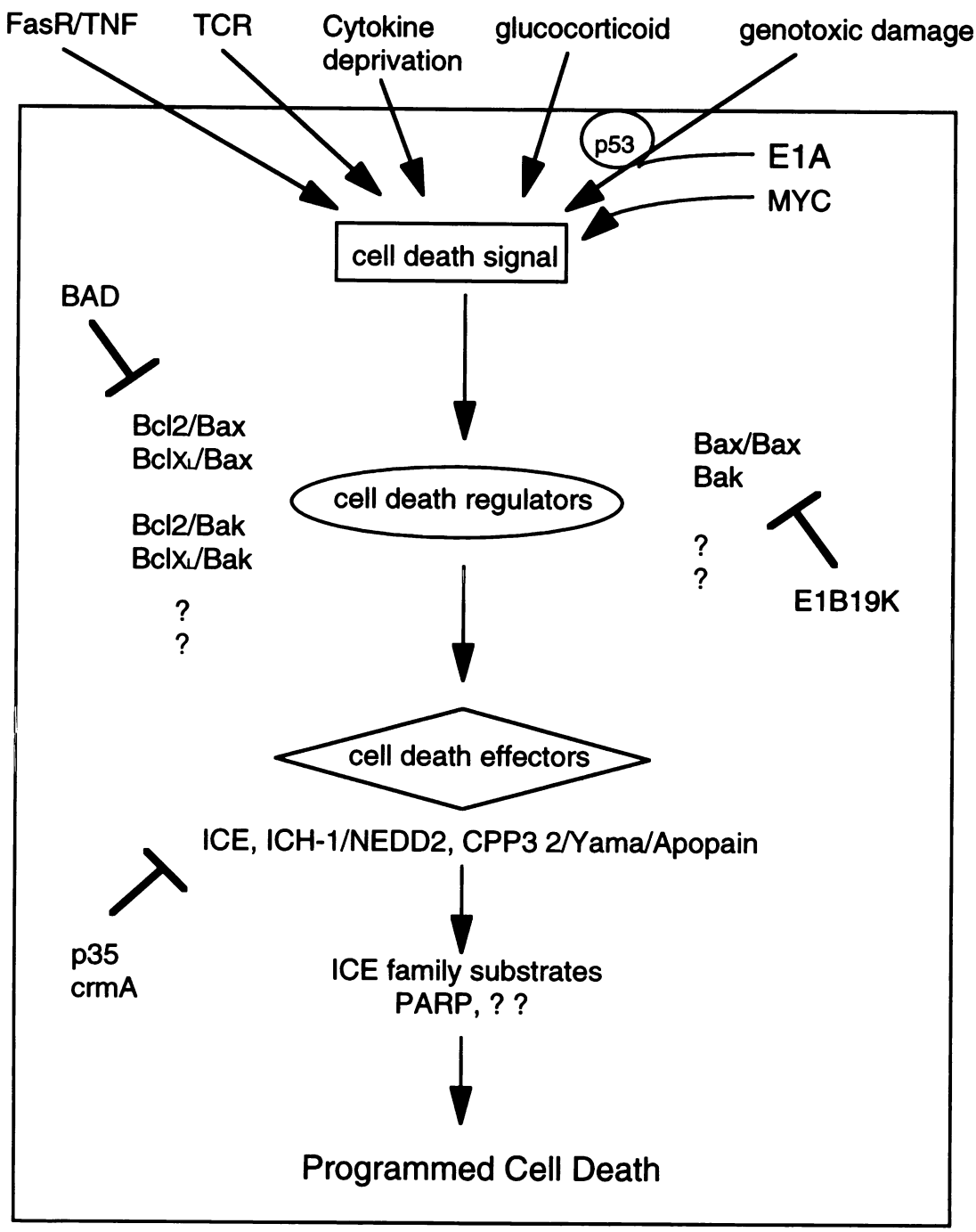
FasR/TNF
TCR
Cytokine deprivation
glucocorticoid
genotoxic damage
p53
E1A
MYC
cell death signal
BAD
Bcl2/Bax
BclXL/Bax
Bcl2/Bak
BclXL/Bak
? ?
cell death regulators
Bax/Bax
Bak
? ?
E1B19K
cell death effectors
ICE, ICH-1/NEDD2, CPP3 2/Yama/Apopain
p35
crmA
ICE family substrates
PARP, ? ?
Programmed Cell Death

individual amino acid residues critical for its activity is described. Peptides corresponding to the N terminus of Bcl2 have also been created and analyzed using circular dichroism (CD) spectroscopy. These results provide new insights into the functional organization of Bcl2 and identify a structural motif that may be prove to be shared by at least a subset of anti-apoptotic proteins.

METHODS

Cell lines -- Human GM701 fibroblasts were grown in Dulbecco's Modified Eagle's medium containing 10% fetal calf serum (FCS), with 100 U/ml penicillin and 0.1 mg/ml streptomycin. Quail QT6 fibroblasts were grown in M199 medium with 5% (v/v) FCS and 1% (v/v) chicken serum. All cells were maintained at 37°C in a 5% CO_2 atmosphere at 90% relative humidity.

Plasmids -- Construction of the Bcl2 vector pSFFV-bcl2, which expresses human Bcl2 using a promoter from the spleen focus-forming virus, has been described previously (17). Mutations were introduced into the Bcl2 coding sequence by oligonucleotide-directed mutagenesis and confirmed by DNA sequencing. A truncated pSFFV-bcl2 mutant, designated ΔAll, lacking all but the first six codons of the *bcl2* sequence, served as negative control (17). The chloramphenicol acetyltransferase (CAT) reporter plasmid pRSV-CAT has been described (17).

Transient-transfection assay for Bcl2 activity -- GM701 cells grown to confluency were split 1:6 into 100-mm plates 24 h before transfection and were then transfected overnight by the calcium phosphate method, with each plate receiving 15 μg wild-type or mutant pSFFV-bcl2, 0.1 μg pRSV-CAT, and 25 μg salmon sperm DNA. Forty hours after transfection, the cells were split 1:2, and one plate from each pair was adjusted to 1 μM staurosporine. Cells were harvested 28 h later and lysed by 3 freeze-thaw cycles in 200 ml 250 mM Tris, pH 7.5. Debris was pelleted by a 5-min microcentrifugation at 4°C, and a 3- to 5-ml aliquot of supernatant was assayed for CAT activity by thin-layer-chromatography and scintillation counting as previously described (17). Survival of cells transfected with a given plasmid was then calculated as the ratio of CAT activity in lysates of staurosporine-treated cells to that in

untreated cells transfected with the same plasmid, expressed as a percentage. The survival of ΔAll-transfected cells depends in part on the duration of staurosporine treatment; in the experiments presented here, it ranged from 2-5%.

Immunoblot assay -- Expression of wild-type and mutant Bcl2 protein was assayed in transiently-transfected quail QT6 fibroblasts using a mouse monoclonal antibody against Bcl2 (DAKO) as described (17). Unlike GM701 fibroblasts, QT6 cells contain no background proteins that cross-react significantly with this antibody.

Peptide synthesis and purification -- The 30-, 21-, and 17-residue Bcl2 peptides were synthesized using standard 1-fluorenylmethoxycarbonyl chemistry and were purified by preparative reverse-phase high-performance liquid chromatography. The N and C termini were unprotected. Their purities were confirmed by analytical reverse-phase chromatography and mass spectral analysis.

Computerized Structural Prediction -- Peptide secondary structure was predicted using computer facilities of the European Molecular Biology Laboratory, Heidelberg and the neural-network algorithm developed by Rost and Sander (20-22). The results were displayed using the facilities of the Computer Graphics Laboratory at UCSF, and the MidasPlus graphics package (Gallo, K., Huang, C., Ferrin, T. E., and Langridge, R. (1989) Univ. of California at San Francisco).

CD spectroscopy -- Samples containing 50 μM peptide were prepared by diluting aliquots of a 1 mM aqueous peptide stock solution with water, 100 mM NaCl, and 200 mM SDS. Samples of the 30-mer peptide were assayed at 15°C at pH 4.0 and pH 7.0, with 20 mM NaCl, 20 mM SDS; the 17- and 21-mer peptides were examined at pH 7.0 only, under the same conditions. A Jasco

J500A CD spectropolarimeter with 1-mm path length cells was used to record each spectrum. Each was the average of 20 scans over the wavelength range of 200-260 nm with a step resolution of 0.4 nm.

RESULTS

This analysis began with the construction of twelve mutant forms of the Bcl2 expression plasmid pSFFV-Bcl2 using oligonucleotide-directed mutagenesis. In each mutant, sequences encoding a pair of adjacent residues in the N-terminal domain were replaced by glycine (or, where glycine was normally present, alanine) codons; together, the mutations spanned the entire 24-amino-acid domain (Fig. 2). To confirm the size and stability of the corresponding mutant proteins, each plasmid was transiently transfected into QT6 avian cells, and extracts from these cells were then examined by immunoblot using a monoclonal antipeptide antibody against Bcl2 residues 41-54. As shown in Fig. 3, each plasmid gave rise to a single immunoreactive peptide of the same apparent mass as the wild-type protein.

A previously described and validated transient transfection assay (17) was then used to test the ability of these Bcl2 mutants to block staurosporine-induced apoptosis in the human fibroblast line GM701, a well-characterized model of apoptosis. In this assay, individual plates of GM701 cells are co-transfected with a wild-type or mutant Bcl2 plasmid along with a CAT reporter plasmid. After a period of growth, each plate is split into treatment and control groups. The latter are exposed to the protein kinase inhibitor staurosporine, which induces apoptosis within 24 h in untransfected GM701 cells and in those cells transfected with nonfunctional Bcl2 mutant. This results in a time-dependent decrease in CAT activity in the treated plate with respect to its untreated counterpart. By contrast, cells transfected with wild-type Bcl2 or with a functional mutant do not undergo apoptosis, and

Figure 2. Schematic depiction of the human Bcl2 protein (above) showing approximate locations of the hydrophobic tail (black) and of two other regions required for anti-apoptotic function (shaded). Wild-type sequence of the N-terminal region is shown (below), along with those of 12 dicodon missense mutants used in this study.

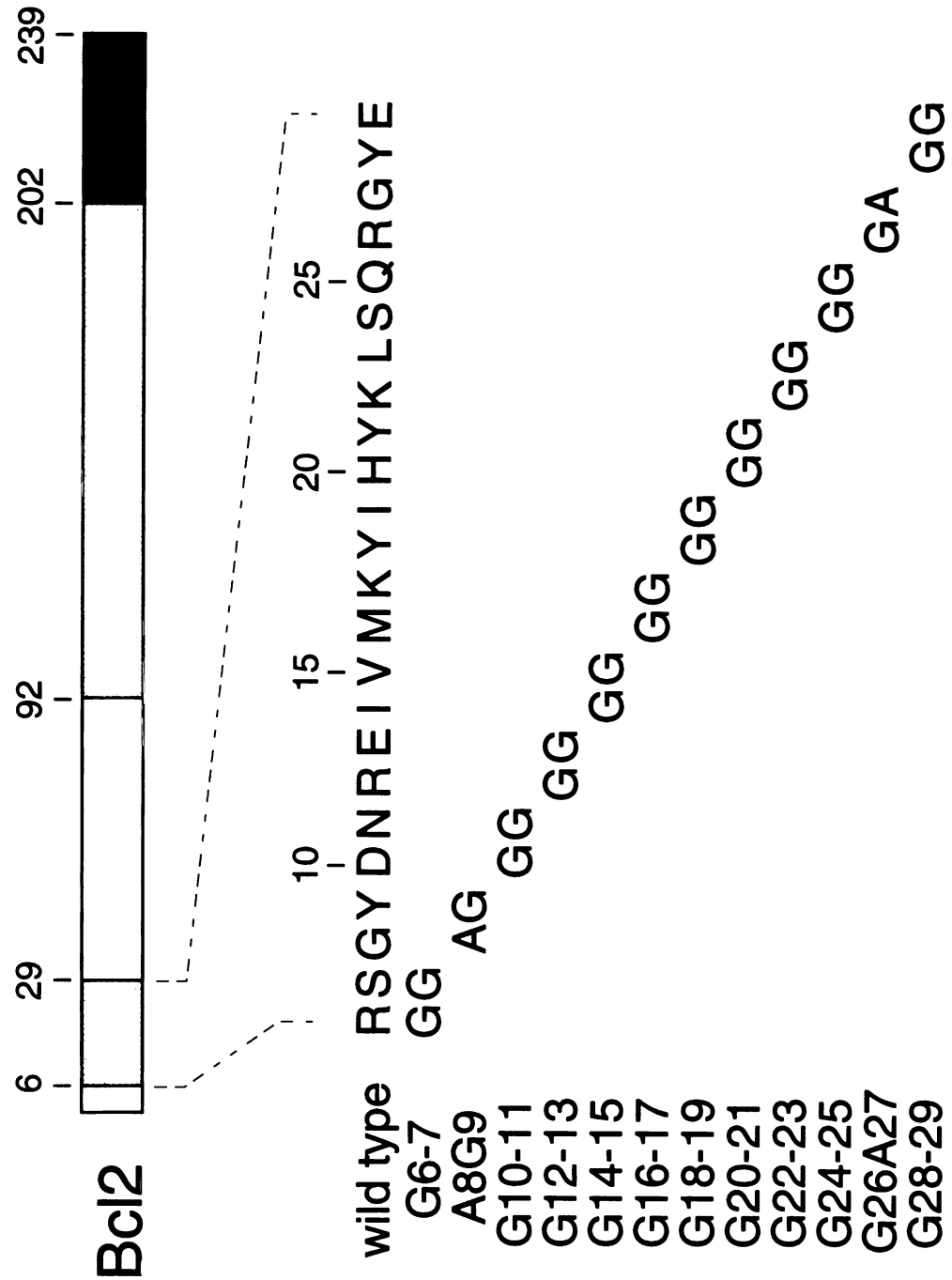
Bcl2
6
29
92
202
239
10
15
20
25
wild type RSGYDNREIVMKYIHYKLSQRGYE
G6-7 GG
A8G9 AG
G10-11 GG
G12-13 GG
G14-15 GG
G16-17 GG
G18-19 GG
G20-21 GG
G22-23 GG
G24-25 GG
G26A27 GA
G28-29 GG

Figure 3. Immunoblot detection of the 12 dicodon Bcl2 mutants in lysates of transiently transfected QT6 cells, using a monoclonal anti-Bcl2 antibody. Each lane contains 10 μg total protein except those for mutants G14-15, G18-19, and G22-23, which contain 20 μg protein. "Neg ctrl," sham-transfected cells; "wt Bcl-2," QT6 cells stably transfected with the Bcl2 expression vector (17).

G6–7
A8G9
G10–11
G12–13
G14–15
G16–17
G18–19
G20–21
G22–23
G24–25
G26A27
G28–29
Neg ctrl
wt Bcl-2

consequently, chloramphenicol acetyltransferase activities within each pair of plates remain more nearly equal (17).

Three mutants involving residues 14-15, 18-19, and 22-23, respectively, were found whose ability to inhibit apoptosis was totally abrogated (Fig. 4). Chloramphenicol acetyltransferase activity was reduced by more than 95% after staurosporine treatment in cells transfected with these mutants, indicating that they conferred almost no protection against apoptosis. The remaining mutants, by contrast, provided levels of protection comparable with that of the wild-type protein: in each case, CAT activity in the drug-treated plates averaged at least 73% that observed in untreated plates. The three inactive mutants were each expressed at levels approximately two-fold lower than those of the other mutants, suggesting either that these mutations partially destabilized the protein or that cells expressing functional Bcl2 have a growth or survival advantage in the transient assay (to compensate for this disparity, two-fold more total protein was loaded for each of these mutants on the gel shown in Fig. 3). However, one other mutant (G24-25) that was expressed at comparably low levels conferred essentially wild-type protection (Figs. 2 and 3), implying that the functional defect in the three inactive mutants was not entirely due to reduced protein expression. This interpretation was borne out in the following experiment.

In order to determine which of the six implicated residues were essential, another series of mutant Bcl2 plasmids that contained glycine-substitution mutations in individual codons was constructed. Immunoblots using the anti-Bcl2 antibody again confirmed the size and stability of each mutant protein (Fig. 5); within this series, the levels of protein expression varied no more than two-fold among mutants. Using the transient transfection assay (Fig. 6), it was found that individual mutations of residues Ile-14, Val-15, Tyr-

Figure 4. Anti-apoptotic activity of the dicodon Bcl2 mutants. Activity is expressed as the percent survival of staurosporine-treated GM701 cells transiently transfected with the indicated mutants, as compared with untreated cells expressing the same mutant (17). In this experiment, transient-transfection of wild-type pSFFV-Bcl2 conferred approximately 100% protection against apoptosis ("wt Bcl-2"), whereas the inactive mutant ΔAll gave <5 % protection (data not shown).

Survival (%)
0.0
0.5
1.0
1.5
G6-7
A8G9
G10-11
G12-13
G14-15
G16-17
G18-19
G20-21
G22-23
G24-25
G26A27
G28-29
wt Bcl2

Figure 5. Immunoblot detection of the six single codon Bcl2 mutants in lysates of QT6 cells using an anti-Bcl2 monoclonal antibody. The first six lanes contain 20, 10, 10, 10, 20, and 15 μg total protein, respectively. "Neg ctrl" and "wt Bcl2" are as described for Fig. 3.

I14G
V15G
Y18G
I19G
K22G
L23G
Neg ctrl
wt Bcl-2

Figure 6. Anti-apoptotic activities of the single codon Bcl2 mutants and of wild-type pSFFV-Bcl2 ("wt Bcl-2") in the transient transfection assay. In this experiment, ΔAll gave ≤ 5 % survival (data not shown).

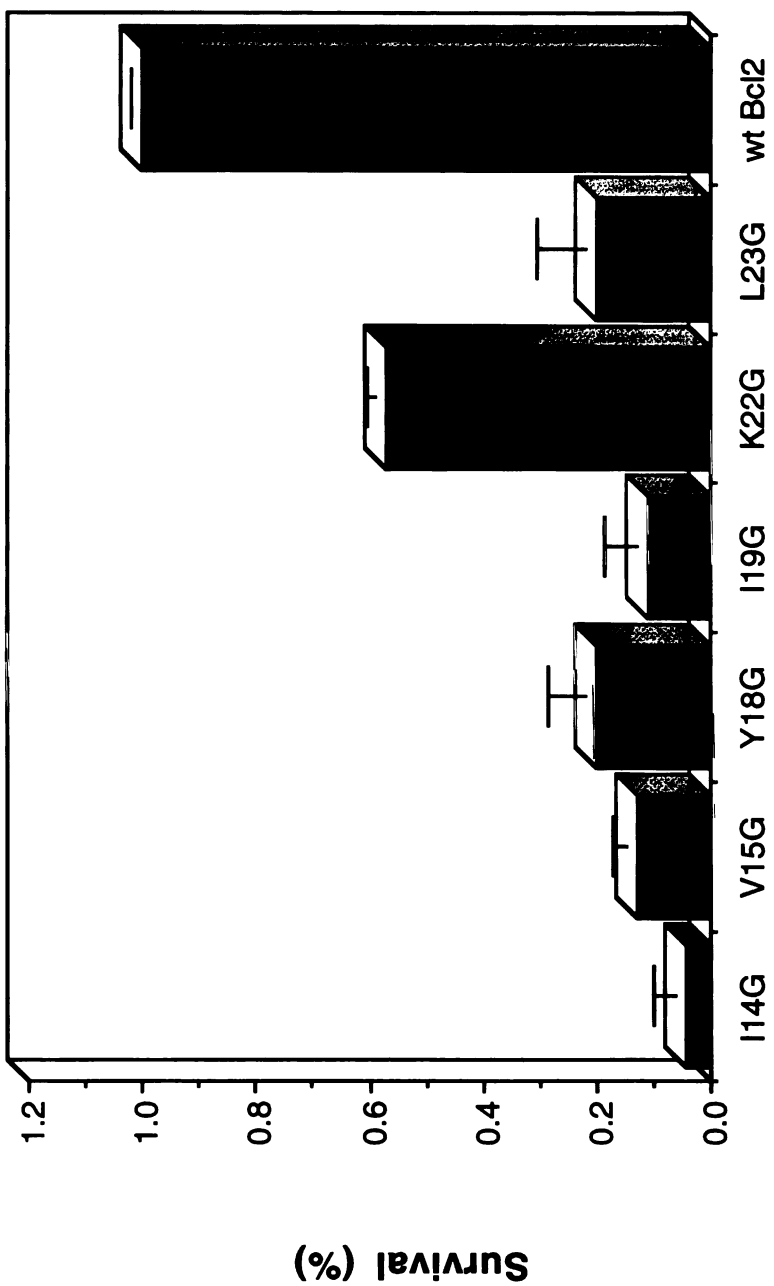
Survival (%)
0.0
0.2
0.4
0.6
0.8
1.0
1.2
I14G
V15G
Y18G
I19G
K22G
L23G
wt Bcl2

18, Ile-19, and Leu-23 each reduced Bcl2 activity by at least 80%. The mutant K22G was less seriously impaired, retaining roughly half the wild-type activity. Together, these results indicated that residues Ile-14, Val-15, Tyr-18, Ile-19, and Leu-23 were indispensible for anti-apoptotic activity of Bcl2, whereas the remaining 19 residues in the N-terminal domain were not specifically required.

Next, the primary sequence of Bcl2 was analyzed using the protein secondary structure prediction algorithm of Rost and Sander (20-22). This method uses a computerized neural-network approach that exploits multiple sequence alignments in both the training and prediction phases, uses a balanced sampling of helical, sheet and coiled structures for training, and evaluates the structural context of individual residues without reference to adjacent sequences. Earlier studies (20,21) indicate that the accuracy of this method in predicting three-state (i.e., helix vs. sheet vs. coil) conformations of known structures is approximately 70%. This algorithm was used to generate structural predictions for the full-length sequence of Bcl2, and also independently for the sequences of residues 2-31, 6-26, and 10-26 in isolation. In every case, the algorithm predicted with at least 72% confidence that residues 11-26 would adopt an α-helical conformation (data not shown). This region of predicted helicity encompassed all five of the residues that had been found to be critical for function. Figures 7A and 7B show two views of a space-filled model of the N-terminal region (residues 2-31) based on this structural prediction, with residues 11-26 modeled as α-helix and residues 2-10 and 27-31 as random coil. In this model, the five critical residues (magenta) are found to be positioned together on one face of the helix.

Figure 7. Predicted conformation of the Bcl2 N terminus. Two perpendicular views are shown of a computer-generated water-accessible surface model of residues 2-31 of human Bcl2, with residues 11-26 in helical conformation. The N terminus is oriented upward in each case; sidechain conformations are arbitrary. Magenta shading indicates the five functionally essential residues identified in this study.

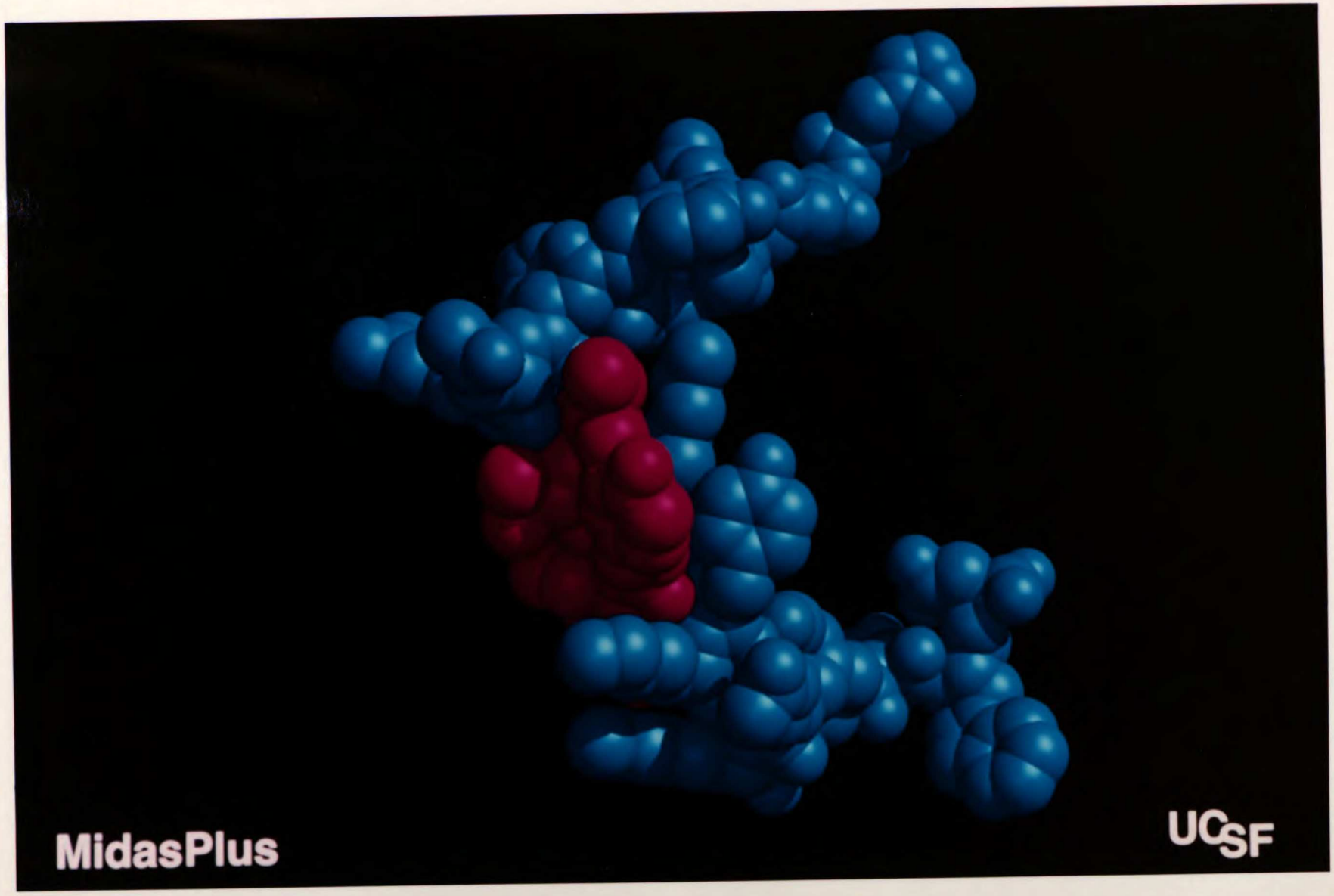
MidasPlus
UCSF


MidasPlus
UCSF

To search for physical evidence of such a helix, a 30-mer peptide corresponding to residues 2-31 of Bcl2 (Fig. 8A) was synthesized. Its conformation in solution was evaluated under different temperatures, pHs, and salt concentrations using CD spectroscopy. In aqueous solution, the peptide exhibited only a single spectral minimum at 198 nm, suggesting a random-coil conformation (data not shown). However, when 20 mM of SDS micelles were added, markedly different spectra that included two minima at 208 nm and 222 nm, respectively (Fig. 8B) were obtained; these features indicate the presence of significant α-helical structure. The extent of helicity, as reflected in the values of these spectral minima, was approximately 27% and seemed similar at pH 4.0 and pH 7.0 (Fig. 8B). Further CD spectra in the presence of SDS suggested that the extent of helicity remained constant as NaCl concentration varied from 0 to 50 mM but decreased with increasing temperature (data not shown).

In an effort to identify the regions of highest helical propensity, two shorter synthetic peptides corresponding to Bcl2 residues 6-26 and 10-26, respectively (Fig. 8A) were then examined. Like the larger peptide, each appeared to be a random coil in the absence of detergent (data not shown), but acquired significant helicity in the presence of 20 mM SDS (Fig. 8C). Of note, the CD spectral minima of the 17-residue peptide were somewhat more negative than those of the larger peptides, suggesting that the region of greatest helical propensity lies, as predicted, within residues 11-26.

Figure 8. CD spectroscopy of N-terminal peptides from Bcl2. **A)** Sequences of the 30-, 21-, and 17-mer peptides used in this study. Location of the predicted helical region (residues 11-26) is indicated above. **B)** CD spectra of the 30-mer peptide in the presence of 20 mM SDS at 15°C, pH 7.0 and pH 4.0. **C)** CD spectra of the three peptides at pH 7.0 in 20 mM MOPS, 20 mM NaCl, 20 mM SDS at 15°C.

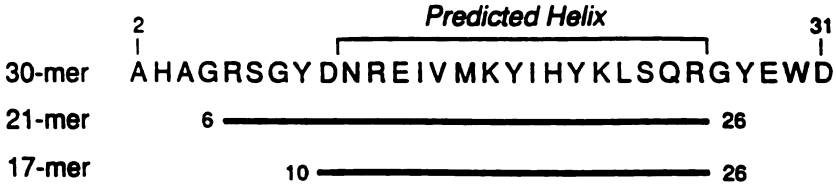
Predicted Helix
2
31
30-mer AHAGRSGY DNREIVMKYIHYKLSQRGYEWD
21-mer 6 26
17-mer 10 26

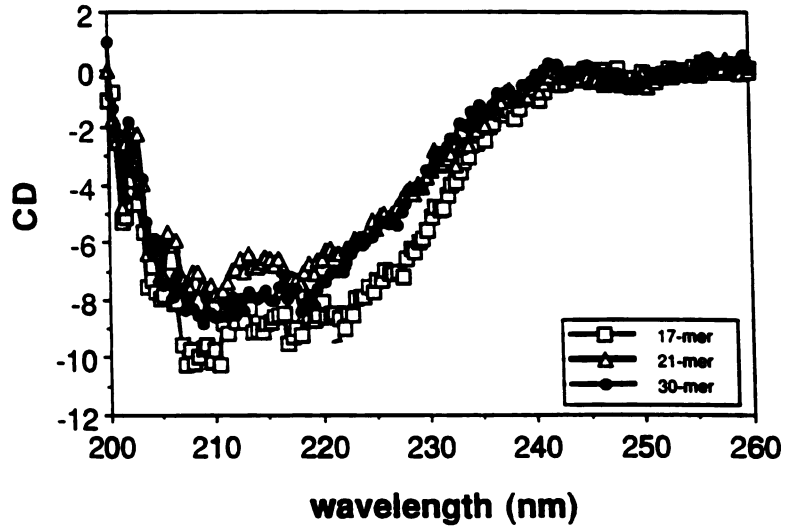
CD
wavelength (nm)
17-mer
21-mer
30-mer

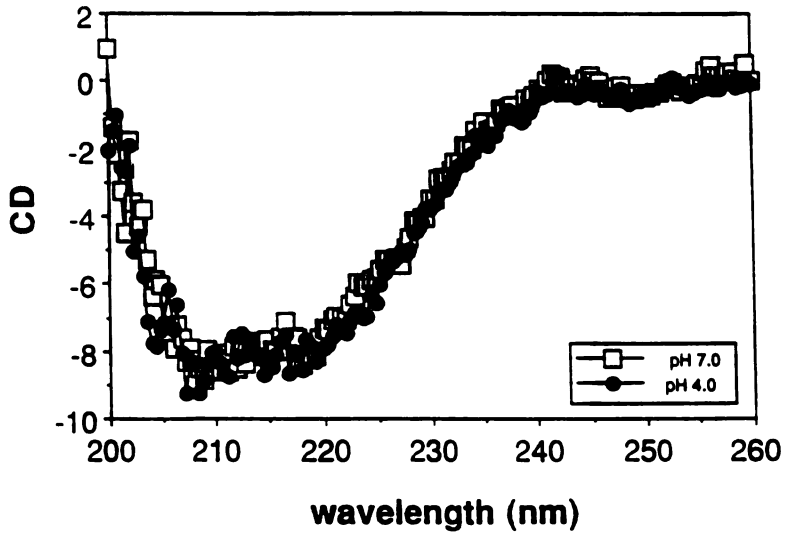
CD
wavelength (nm)
pH 7.0
pH 4.0

DISCUSSION

Sequence comparisons among Bcl2 proteins from various species reveal a cluster of conserved residues corresponding to positions 6-29 in the human protein (3). Deletion of this region eliminates the ability of Bcl2 to prevent apoptosis, even when expressed at high concentration (16,17,19); the importance of this region has been demonstrated in several different cell types undergoing apoptosis in response to diverse stimuli. By contrast, the adjacent residues 30-79 have diverged widely in evolution and can be deleted with only a modest decrement in Bcl2 activity (17). These observations imply that the N-terminal region plays an essential role in Bcl2 function. In the present study, a more detailed mutational analysis to map the essential features of this region was conducted, and it was found that only five specific amino acid residues within it -- Ile-14, Val-15, Tyr-18, Ile-19, and Leu-23 -- are essential for anti-apoptotic activity. Individual mutations in any one of these five hydrophobic or aromatic residues profoundly inhibited Bcl2 activity in a transient transfection assay, whereas every other residue could be replaced by glycine or alanine without more than 50% loss of activity.

The periodic spacing of the critical residues, coupled with a computerized structural prediction for the entire N-terminal region, suggested that this region might be α-helical. Additional support for this conjecture was obtained from CD spectral analysis, which revealed that peptides encompassing the critical sequences from the Bcl2 N terminus readily adopt a helical conformation in the presence of SDS micelles -- conditions which may be presumed to mimic the amphiphilic environment found at hydrophobic surfaces of cellular membranes or in the cores of globular proteins (23-27). Provided that such micelles (or other hydrophobic reagents such as TFE) were

present, the peptides maintained their helical properties across a fairly broad range of pH and salt concentration. The fact that this helical folding occurred in the absence of flanking peptide sequences, coupled with the evidence that deleting residues 30-79 from Bcl2 has only minimal effect on its activity (17), suggests that residues 6-29 might constitute an autonomous structural domain. Modeling of this domain further suggests that its function may depend upon clustering of the five critical hydrophobic and aromatic residues on one surface of the helix, as depicted in Fig. 7.

Indirect evidence for α-helix formation in the N terminus of Bcl2 comes from X-ray crystallographic and nuclear magnetic resonance (NMR) spectroscopic studies of the Bcl2 homologue, $BclX_L$ (28). It is well known that homologous proteins have the same three-dimensional fold and approximately equal secondary structures down to a level of 25-30% identical residues (29). $BclX_L$, which is functionally similar to Bcl2, displays 44% amino acid identity to Bcl2, with the areas of highest homology or identity encompassing the highly conserved BH1 and BH2 domains as well as the N terminus. The high degree of sequence homology between $BclX_L$ and Bcl2 suggest that these proteins might exhibit a similar fold. Therefore, the demonstration of an amphipathic helix within the N terminus of $BclX_L$ by both X-ray crystallography and NMR spectroscopy corroborates the finding of α-helicity in the N-terminal region of Bcl2 reported here.

Though the biological role of this apparently helical domain is not yet known with certainty, one possibility is that its hydrophobic surface mediates contacts either within or between proteins. Such contacts might, for example, be necessary for proper folding of the Bcl2 monomer, or for interaction with other protein components of the apoptotic pathway. Support for the idea that this domain might be important for stabilizing the structure of the

monomeric protein comes from the demonstration that the N-terminal helix of $BclX_L$ seems to have extensive hydrophobic interactions with its two central helices as well as one of its flanking amphipathic helices (28). An alternative, though not mutually exclusive, hypothesis is that this domain helps mediate the formation of oligomers or higher multimers of Bcl2 within cells. Support for the latter hypothesis comes from studies by Reed and co-workers (18,19) which indicate that Bcl2 may homomultimerize through sequential "head-to-tail" contacts between N-terminal and C-terminal sequences of consecutive monomers. According to this model, Bcl2 variants that carry mutations or deletions affecting the critical N-terminal residues would retain the ability to dimerize with wild-type Bcl2 (as they have been observed to do, see refs. 17-19), but would be unable to form higher multimers. Presuming that multimerization is essential for Bcl2 function, this might, in turn, account for the inability of such mutants to protect against apoptosis. Moreover, because incorporation of even one such mutant would block the formation of a wild-type multimer through chain-termination, this model would also account for the finding that N-terminal Bcl2 mutants exert their dominant negative effects even at relatively low molar ratios (near 1:1) of mutant to wild-type protein (17). Activity at such low stoichiometric ratios is in fact typical of dominant negative mutants that act by blocking formation of higher-order multimers (30-32).

Amino acid sequence comparisons suggest that analogues of the critical five-residue motif from Bcl2 may also be present in at least some related proteins. Earlier published alignments (e.g., ref. 3) have identified regions resembling the Bcl2 N terminus in the anti-apoptotic proteins $BclX_L$, A1, and Ced-9, as well as in the pro-apoptotic protein Bax. Those analyses, however, were based on the entire N-terminal sequence, and so include a

preponderance of residues that are not specifically required for function. Re-evaluation of the alignments focusing only on the critical residues identified in this study (Fig. 9) reveals that the five-residue motif is well conserved in $BclX_L$ and A1. Moreover, the five-residue motif lies within the N-terminal helix of $BclX_L$ (28), and an analysis of potential secondary structure in the A1 protein using the Rost and Sander algorithm suggests that the conserved residues lie within a region of predicted α helix (data not shown) in A1, thus strengthening the apparent resemblance to the Bcl2 motif. Less satisfactory sequence matches may also be present in the nematode Ced-9 and Epstein-Barr virus BHRF1 proteins, but these were not predicted to lie within regions of helicity, and so may not be true counterparts of the Bcl2 N-terminal motif. Most importantly, no sequences matching this motif could be identified anywhere within Bax, Bak, or Bad -- three Bcl2-related proteins that promote, rather than antagonize, apoptosis. By contrast, close homologues of the BH1 and BH2 motifs are present in all three of these proteins (6-10). Taken together, these results suggest that the functional domain at the N terminus of Bcl2, which consists of a putative α-helix bearing five critical spaced hydrophobic and aromatic residues, may have counterparts in at least a subset of related anti-apoptotic proteins, and that its presence distinguishes these from related proteins which act to favor programmed cell death.

Figure 9. N-terminal sequence alignments for selected members of the Bcl2 protein family. The alignments shown are from ref. 3, and represent the maximal global similarities to residues 10-28 of human Bcl2; dots indicate gaps introduced to optimize the alignments. Solid rectangles enclose the five critical residues identified in this study for Bcl2, and corresponding residues in $BclX_L$ (5) and A1 (33). Dashed rectangles indicate possible counterparts of these residues in the nematode Ced-9 and Epstein-Barr virus Bhrf-1 proteins. No convincing match to this 5-residue motif was detected in Bax, nor in Bad or Bak (data not shown).

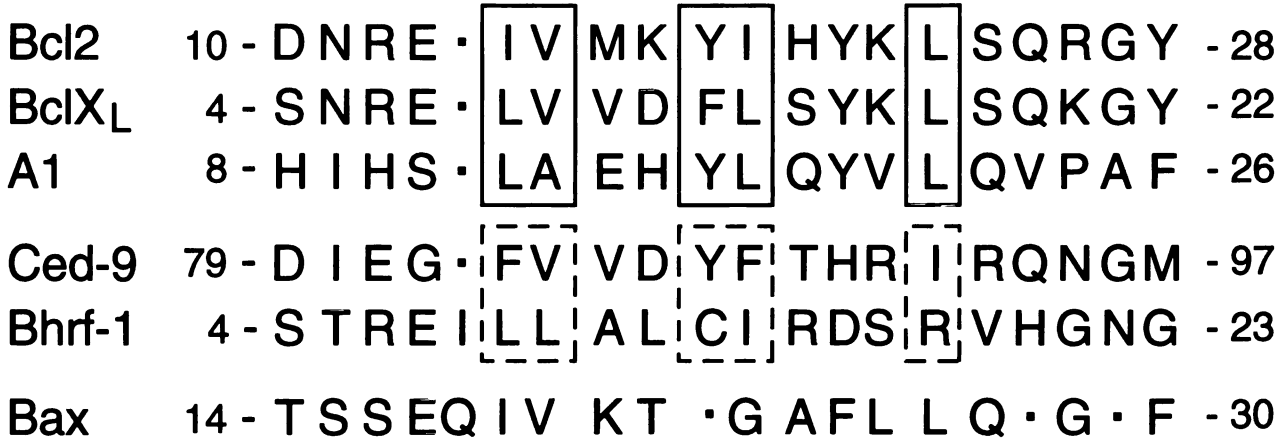
Bcl2 10 - D N R E · I V M K Y I H Y K L S Q R G Y - 28
BclX$_L$ 4 - S N R E · L V V D F L S Y K L S Q K G Y - 22
A1 8 - H I H S · L A E H Y L Q Y V L Q V P A F - 26
Ced-9 79 - D I E G · F V V D Y F T H R I R Q N G M - 97
Bhrf-1 4 - S T R E I L L A L C I R D S R V H G N G - 23
Bax 14 - T S S E Q I V K T · G A F L L Q · G · F - 30

BIBLIOGRAPHY

1. Ellis, R. E., Yuan, J., and Horvitz, H. R. (1991) *Annu. Rev. Cell Biol.* **7**, 663-698
2. Jacobson, M.D., Burne, J.F., Raff, M.C. (194) *EMBO J.* **13**, 1899-1910
3. Cory, S. (1995) *Annu. Rev. Immunol.* **13**, 513-544
4. Reed, J. C. (1994) *J. Cell Biol.* **124**, 1-6
5. Boise, L. H., González-García, M., Postema, C. E., Ding, L., Lindsten, T., Turka, L. A., Mao, X., Nuñez, G., and Thompson, C. B. (1993) *Cell* **74**, 597-608
6. Oltvai, Z. N., Milliman, C. L., and Korsmeyer, S. J. (1993) *Cell* **74**, 609-619
7. Yang, E., Zha, J., Jockel, J., Boise, L. H., Thompson, C. B., and Korsmeyer, S. J. (1995) *Cell* **80**, 285-291
8. Farrow, S. N., White, J. H. M., Martinou, I., Raven, T., Pun, K.-T., Grinham, C. J., Martinou, J.-C., and Brown, R. (1995) *Nature* **374**, 731-733
9. Chittenden, T., Harrington, E. A., O'Connor, R., Flemington, C., Lutz, R. J., Evan, G. I., Guild, B. C. (1995) *Nature* **374**, 733-736
10. Kiefer, M. C., Brauer, M. J., Powers, V. C., Wu, J. J., Umansky, S. R., Tomei, L. D., and Barr, P. J. (1995) *Nature* **374**, 736-739
11. Yin, X. M., Oltvai, Z. N., and Korsmeyer, S. J. (1994) *Nature* **369**, 321-323
12. Oltvai, Z. N., and Korsmeyer, S. J. (1994) *Cell* **79**, 189-192
13. Vaux, D.L., Cory, S., Adams, J.M. (1988) *Nature* **335**, 440-42
14. Sentman, D. L., Shutter, J. R., Hockenbery, D., Kanagawa, O., Korsemeyer, S. J. (1991)*Cell* **67**, 879
15. Vaux, D. L., Aguila, H. L., Weissman, I. L. (1992) *Int Immunol* **4**, 821
16. Borner, C., Martinou, I., Mattmann, C., Irmler, M., Schaerer, E., Martinou, J.-C., and Tschopp, J. (1994) *J. Cell Biol.* **126**, 1059-1068

17. Hunter, J. J., Bond, B. L., and Parslow, T. G. (1996) *Molec. Cell. Biol.* **16**, 877-83

18. Sato, T., Hanada, M., Bodrug, S., Irie, S., Iwama, N., Boise, L. H., Thompson, C. B., Golemis, E., Fong, L., Wang, H.-G., and Reed, J. C. (1994) *Proc. Natl. Acad. Sci. U.S.A.* **91**, 9238-9242

19. Hanada, M., Aimé-Sempé, C., Sato, T., and Reed, J. C. (1995) *J. Biol. Chem.* **270**, 11962-11969

20. Rost, B., and Sander, C. (1993) *J. Mol. Biol.* **232**, 584-599

21. Rost, B., and Sander, C. (1994) *Proteins* **19**, 55-72

22. Rost, B., Sander, C., and Schneider, R. (1994) *Comp. Appl. Biosci.* **10**, 53-60

23. Pervushin, K. V., Arseniev, A. S., Kozhich, A. T., and Ivanov, V. T. (1991) *J. Biol. NMR* **1**, 313-322

24. Rizo, J., Blanco, F. J., Kobe, B., Bruch, M. D., and Gierasch, L. M. (1993) *Biochemistry* **32**, 4881-4894

25. Backlund, B.-M., Wikander, G., Peeters, T. L., and Gräslund, A. (1994) *Biochim. Biophys. Acta* **1190**, 337-344

26. Killian, J. A., Trouard, T. P., Greathouse, D. V., Chupin, V., Lindblom, G. (1994) *F.E.B.S. Lett.* **348**, 161-165

27. Zhang, H., Kaneko, K., Nguyen, J. T., Livshits, T. L., Baldwin, M. A., Cohen, F. E., James, T. L., and Prusiner, S. B. (1995) *J. Molec. Biol.* **250**, 514-526

28. Muchmore, S.W., et al. (1996) *Nature* **381**, 335-341

29. Chothia, C. and Lesk, A. M. (1986) *EMBO J.* **5**, 823-826.

30. Waterston, R. H., Hirsh, D., and Lane, T. R. (1984) *J. Molec. Biol.* **180**, 473-496

31. Herskowitz, I. (1987) *Nature* **329**, 219-222

32. Trono, D., Feinberg, M. B., and Baltimore D. (1989) *Cell* **59**, 113-120

ACKNOWLEDGMENTS

This work was supported in part by Grants AI29313 and AI36636 from the National Institutes of Health and by a medical student research fellowship from the Howard Hughes Medical Institute.

I would like to thank John J. Hunter, Anwer Mujeeb, Christoph Turck, and Tristram G. Parslow for all their guidance and support.

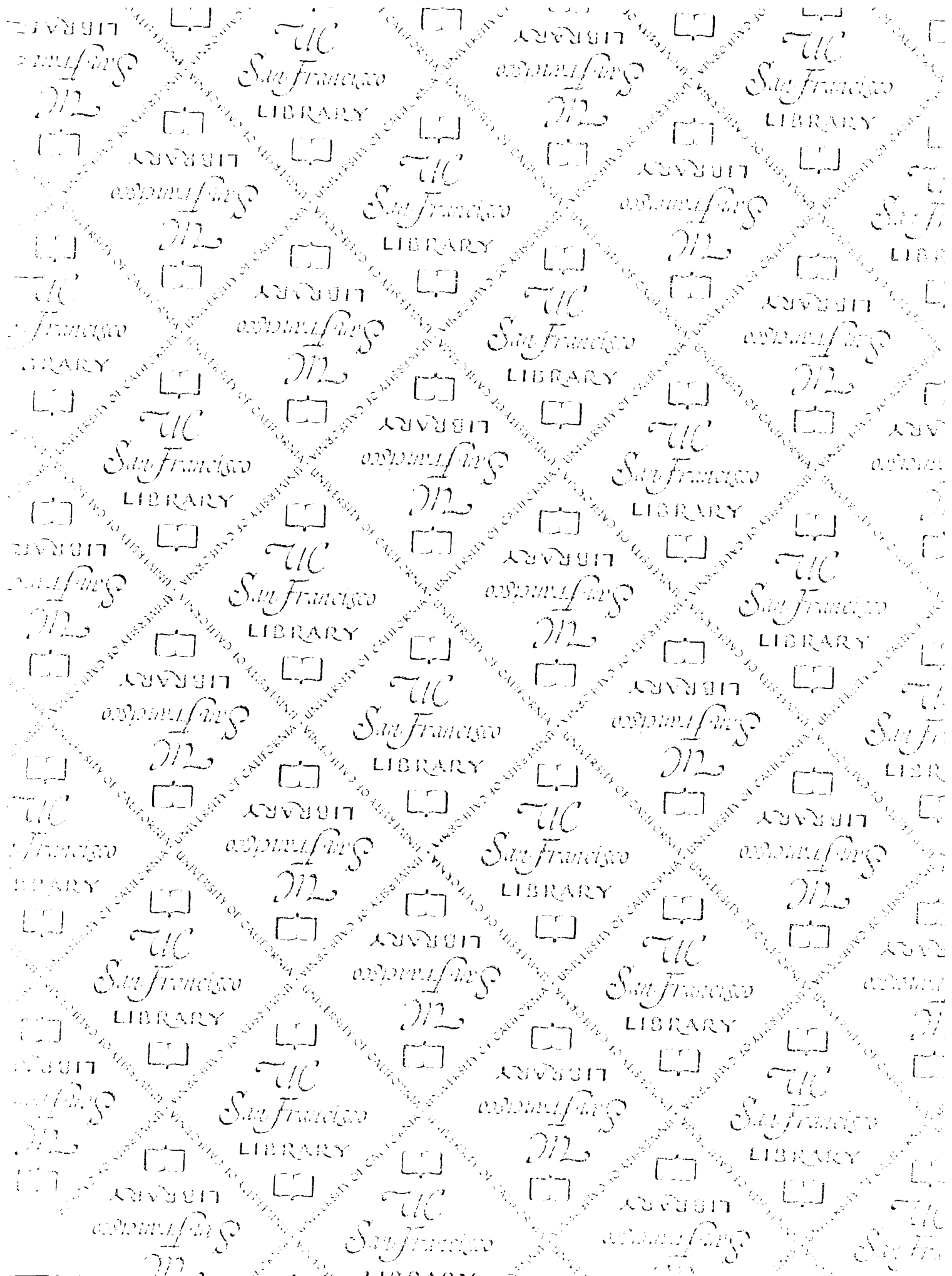
UC
San Francisco
LIBRARY


For reference
Not to be taken from the room.
SF Library